Complexation of NdI_3 – LiI in the Gaseous and Molten States

TRYGVE FOOSNÆS * and HARALD A. ØYE **

Institutt for uorganisk kjemi, Norges tekniske høgskole, Universitetet i Trondheim, N-7034 Trondheim-NTH, Norway

The equilibrium between liquid mixtures of NdI_3 – LiI and their vapor phase has been studied by means of absorption spectroscopy of the gas phase. In the temperature range 1100–1250 K, the gas phase can be described by the equilibrium

$$NdI_3(g) + LiI(g) = LiNdI_4(g)$$
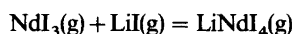
with $\Delta H° = -210 \pm 2$ kJ/mol and $\Delta S° = -115 \pm 3$ J/mol K. The liquid phase is described by the equilibrium between three different types of I^- ions:

$$2[-\overset{|}{\underset{|}{Nd}}-I]^{-0.5} = [-\overset{|}{\underset{|}{Nd}}-I-\overset{|}{\underset{|}{Nd}}-]+I^-$$
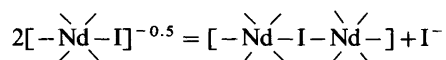
with $K = 1.5$.

The present work was aimed at studying gas complexation above liquid mixtures with different composition. From the determination of the absorption spectra of the gas phase,[1] it is possible to obtain structural and thermodynamic information of the gaseous as well as the liquid phase.

Gas complexation specially with group III metal halides has received considerable attention lately and four reviews [2-5] give a survey of the recent work. The system LiI – NdI_3 was chosen for the present study. Apart from the fundamental interest, systems like this play an important part in multi-vapor lamps when iodide mixtures are added in order to improve energy efficiency and color rendering properties of the emitted light.[6,7] Although the light emitting arc may have a temperature of 3000–6000 K, the amount of salt vapor to enter the gas phase will be determined by an equilibrium with a molten salt pool with temperatures in the range 1000–1300 K. The liquid pool is situated on the lamp wall.

Absorption spectra of gaseous $NdBr_3$ and NdI_3 have been measured by Gruen and DeKock.[8] The absorption bands of Nd^{3+} are due to electronic transitions within the 4f configurations. For the $^4I_{9/2}$ – $^4G_{5/2}$ transition between 16 and 17 kK, molar absorptivities of 345 and 116 l/mol cm were measured for $NdI_3(g)$ and $NdBr_3(g)$, respectively. The increase in the molar absorptivity in going from $NdBr_3(g)$ to $NdI_3(g)$ was attributed to increasing covalency in the chemical bonds.

The formation of complexes in the equilibrium vapor above liquid mixtures of CsI – LaI_3, MI – CeI_3, CsI – NdI_3, MI – SmI_2 and MI – ScI_3 (MI = alkali iodide) has been investigated by Liu and Zollweg,[9] and Hirayama, Liu and Zollweg,[10] using mass spectrometry, absorption spectroscopy, vapor pressure measurements by the boiling point method and vapor transpiration techniques. The dominant vapor species was found to be $MLnI_4$ (Ln = lanthanide element), and it was observed that the gas complex was formed more readily with CsI than with NaI.

In the SmI_2-binaries, the tendency to form 1:1 complexes was weak, and $NaSmI_3$ could not be detected in the NaI – SmI_2 system. In the NaI – ScI_3 system, minor amounts of Na_2ScI_5 were found together with $NaScI_4$ in the vapor. At 1000 K the complex formation resulted in a volatility enhancement for the lanthanide triiodides of approximately four. For the dissociation of gaseous complexes to MI(g) and $LnI_3(g)$, values for $\Delta H°$ of 356, 280 and 238 kJ/mol were determined for $NaScI_4$, $CsCeI_4$ and $CsNdI_4$, respectively. The entropy change of the reactions is approximately 125 J/mol K.

* Present address: Chemistry Division, Argonne National Laboratory, Argonne, Ill. 60439, U.S.A.
** Present temporary address: F. J. Seiler Research Laboratory, US Air Force Academy, Col. 80840, U.S.A.

The liquid-vapor equilibria in the systems MCl − LnCl$_3$, where M = Na, K, Cs and Ln = La, Ce, Pr, Nd, Er, have been investigated by Novikov and Gavryuchenkov[11,12,13] and Novikov and Baev.[14] The methods of investigation were vapor pressure measurements by the boiling point method, chemical analysis of the condensed equilibrium vapor and mass spectrometric analysis of the vapor phase. For all systems, the complex formation could be described in terms of formation of MLnCl$_4$(g). The thermodynamic characteristics of the dissociation of MLnCl$_4$(g) show that the stabilities of the complexes are similar. However, for the same lanthanide chloride, there is a weak tendency of decreasing stability of the complex when the alkali chloride is changed from NaCl to CsCl. The measurements also indicate a decreasing stability of the vapor complex for a fixed alkali chloride when the lanthanide chloride is changed in the sequence LaCl$_3$ − ErCl$_3$.

PRINCIPLES

The principle and thermodynamics of high-temperature gas-complex formation investigated by the absorption spectroscopic method are described by Øye and Gruen,[5] and are briefly summarized below.

The system under study, MX$_a$ − M'X$_b$, is contained in closed optical cells. When the sample is heated, M − M' − X species are formed in the vapor phase. In order to determine the partial pressure of the complex species, the molar absorption coefficient of the complexed M^{a+} ion at a specific wave number has to be established. This is done by measuring the optical density in experiments where a small amount of MX$_a$ in the cell is completely evaporated and bound as complex. At a certain wave number v_j the molar absorption coefficient of the complex can be calculated from Beer's law, eqn. (1), when it is assumed that the amount of

$$\varepsilon_c(v_j) = \frac{A(v_j)V}{nl} \tag{1}$$

uncomplexed MX$_a$(g) is negligible. If this assumption does not hold, the value calculated from eqn. (1) must be corrected for the contribution from MX$_a$(g). This case will be treated later.

When the molar absorption coefficient of the complex at v_j is known, the partial pressure of the complex species can be determined in experiments where the vapor is in equilibrium with a condensed phase.

$$P_c = \frac{A(v_j)R\bar{T}}{\varepsilon_c(v_j)l} \tag{2}$$

Eqn. (2) is derived from eqn. (1) by introducing the ideal gas law and solving for P_c. In eqns. (1) and (2)

P_c	= partial pressure of gaseous complex (atm) (1.01325 × 10^5 Pa = 1 atm)
$A(v_j)$	= measured optical density at wave number v_j
R	= gas constant (1 atm/mol K)
$\bar{T}$	= average temperature in the cell (K)
l	= optical path length (cm)
V	= volume of the cell (1)
n	= number of mol of gas complex.

EXPERIMENTAL

Apparatus. The absorption cells used in this work were made of silica tubes (wall thickness 1 − 3 mm, inner diameter 15 − 40 mm) with polished disks of optical quality as windows ("Spectrosil", Thermal Syndicate, Ltd., Wallsend, England). Prior to use, all cells were annealed in a furnace by rapidly increasing the temperature to 1150 °C and cooling slowly to less than 200 °C over a 24 h period. The cell volumes were determined by pycnometric weighing, and the optical path lengths were measured with a caliper.

A horizontal, Kanthal wound, three zone cylindrical furnace was used. The temperature in the furnace was controlled to ±0.1 °C by a Eurotherm PID regulator (Eurotherm Ltd., Sussex, England), with the control thermocouple placed close to the windings of the heating element. The temperature in the middle zone of the furnace was kept lower than in the end zones by adjusting a resistor shunting the middle zone of the heating element, and this prevented condensation of the gas on the cell windows. The temperature profile through the furnace was measured at different controller settings along the axis of a dummy cell with the same optical path length as the actual cells. The temperature was measured near the middle of the cell close to the outside cell wall. A rigid ceramic cell holder with radiation shields was used to keep the cell in the same position in the tube and to reduce heat losses. During runs the temperature profile was the same in each experiment.

The spectrophotometer used was a CARY 17H automatic recording spectrophotometer (Cary Instruments, Monrovia, California). The signals from the spectrophotometer were recorded on a Kennedy Incremental 1600 magnetic tape recorder (Kennedy Co., Altadena, California) via an interfacing unit.[15] The standard deviation in the optical density has been measured to be 2.2×10^{-3} absorption units with this recording system.

Chemicals. The chemicals used were I_2 (E. Merck AG, Germany, doppelt sublimiert), $LiI \cdot 2H_2O$ (Riedel-de Häen AG, Germany) and Nd (Koch Light Laboratories, Ltd., England).

Neodymium triiodide was prepared by reacting Nd metal with I_2 gas in sealed quartz ampoules. The metal was cut in small pieces, washed with acetone and dried under vacuum. Stoichiometric amounts of I_2 were transferred to the reaction tube, and a quartz crucible containing the metal was added. The tube was sealed, and the metal was spread over a large area in one end of the tube. The ampoule was placed in a horizontal quartz furnace with three heating zones. The part of the furnace which contained the iodine was held at $180-190\,°C$, and the temperature in the metal zone was $800\,°C$. The reaction was complete when the iodine color had disappeared. NdI_3 was then sublimed in new quartz ampoules at $600\,°C$ three to four times.

Lithium iodide was prepared by dehydrating $LiI \cdot 2H_2O$. Drying was continued at $300\,°C$ and 10^{-8} atm for 24 h and LiI was finally filtered and recrystallized from the melt.

Procedure. The procedure for charging the cells as described elsewhere[16] was followed with minor differences. The absorption cells were cleaned in ethanol and distilled water, before burning away residual carbon impurities with a torch and a stream of oxygen or compressed air in the cell. Before charging, the cells were evacuated to less than 10^{-8} atm for several hours. The required amounts of salt were weighed out on a balance in a glovebox (H_2O content < 1 ppm) and transferred to the cell through a side arm. For the molar absorptivity experiments the accurate weight was determined by differential weighing. The absorption cells were evacuated to approximately 6×10^{-9} atm at $300\,°C$ for 12 h after charging to remove possible iodine impurities before sealing.

Due to an observed reaction between NdI_3 and the quartz cell, it was decided not to wait for a constant temperature to be established in the furnace during the molar absorptivity measurements. The cells were placed in the furnace at $600\,°C$, and the temperature was immediately increased. The spectral range $700-500$ nm was repeatedly scanned as fast as possible. However, the scan speed was slow enough to properly record the absorption band. With this technique, one spectrum

was recorded each $4-5$ min. The molar absorptivity experiments were normally terminated after three hours.

In experiments performed with the vapor in equilibrium with a condensed phase, equilibrium was established approximately two hours after a change in temperature. The optical density recorded at a fixed wave length as function of time was then constant.

The data recording system and the computer programs enable smoothing of the spectra, drawing the entire or parts of a spectrum to a desired size and subtracting background curves from an observed spectrum. The background has been subtracted in most experiments, and was usually recorded below $200\,°C$, where absorption due to vapor complexes or compounds could not be detected.

A special procedure was necessary in order to determine the molar absorption coefficient of the $Nd-Li-I$ gas complex at the wave number of maximum optical density. Spectra recorded in a molar absorptivity experiment are shown in Fig. 1. The composite band between 16 and 17 kK originates from transitions in the vapor complex, and from transitions in $NdI_3(g)$ in equilibrium with the complex. The net molar absorption coefficient of
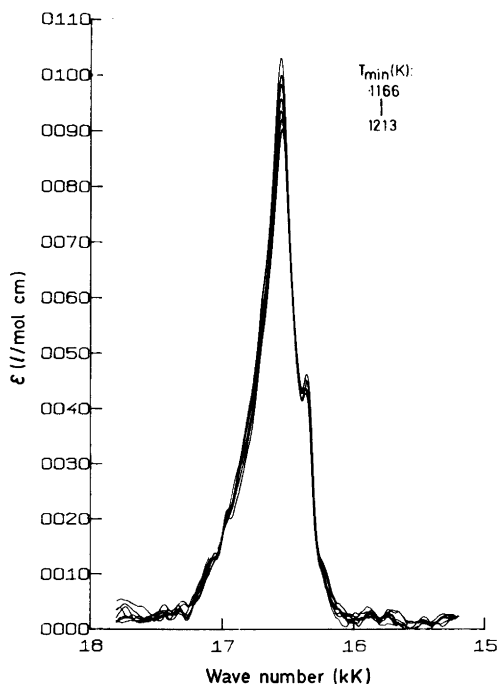

Fig. 1. Molar absorption coefficient of $Nd-Li-I$ gas complex recorded in exp. 5. $T_{min}(K)=1166.5$, 1171.7, 1182.6, 1190.7, 1197.2, 1207.3, 1213.4.

the gas complex is obtained after resolution of the spectra.

The net molar absorption coefficient of the gas complex can be found by introducing the quantity χ [eqn. (3)], where χ defines the ratio of the number of

$$\chi = n_{NdI_3}/n^\circ_{NdI_3} \tag{3}$$

mol of $NdI_3(g)$ in equilibrium with the vapor complex to the total number of moles of NdI_3 in the molar absorptivity cell. The net molar absorption coefficient of the complex at the wave number of maximum optical density, v_j, is then obtained with eqn. (4), where $\varepsilon(v_j)$ is the apparent molar absorption

$$\varepsilon_c(v_j) = \frac{\varepsilon(v_j) - \chi\varepsilon_{NdI_3}(v_j)}{1-\chi} \tag{4}$$

coefficient and $\varepsilon_{NdI_3}(v_j)$ is the molar absorption coefficient of NdI_3 at wave number v_j. The spectra were resolved by a trial and error method, using a graphical terminal. This method is based on the observations that the absorption spectrum of pure $NdI_3(g)$ in equilibrium with $NdI_3(l)$ has the same appearance at all temperatures, except for the intensities, and that the absorption maxima are centered at the same wave numbers at all
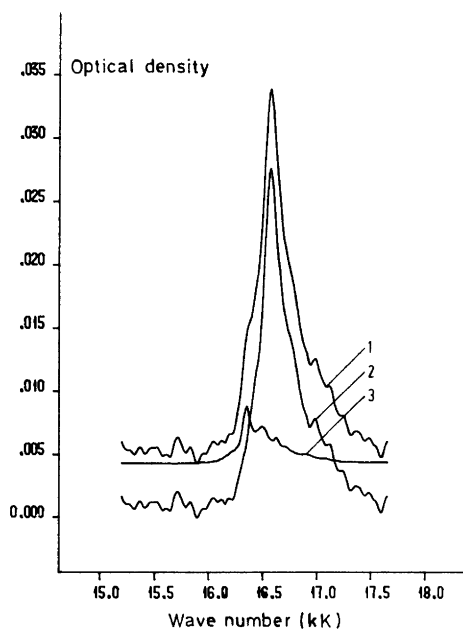
temperatures. Thus, one of the recorded spectra of $NdI_3(g)$ may serve as a reference spectrum. The optical density at each wave number in the reference spectrum is multiplied by a scaling factor chosen by the user, and the result is subtracted from the composite spectrum.

The difference spectrum that results from this calculation is displayed on the terminal screen. A new scaling factor may be entered, and the calculation repeated. The numerical value of the scaling factor that is accepted gives a difference spectrum that is a smooth curve for wave numbers where NdI_3 has absorption maxima. An example of this band resolution technique is shown in Fig. 2.

When the scaling factor k has been obtained from the resolved spectrum, χ is calculated from eqn. (5),

$$\chi = \frac{n_{NdI_3}}{n^\circ_{NdI_3}} = \frac{kA_{ref}(v_j)V}{\varepsilon_{NdI_3}(v_j)ln^\circ_{NaI_3}} \tag{5}$$

which is derived by introducing eqn. (1) in eqn. (3). $A_{ref}(v_j)$ is the optical density measured at v_j for $NdI_3(g)$ in a separate reference experiment, V and l are the volume and optical path length of the molar absorptivity cell and $\varepsilon_{NdI_3}(v_j)$ is the molar absorptivity of $NdI_3(g)$ at v_j. With this resolving procedure, differences in the scaling factor of ± 0.01 could be distinguished.

RESULTS AND DISCUSSION

A. Molar absorption coefficient of the Nd−Li−I gas complex

The apparent molar absorption coefficient at the wave number of maximum optical density (16.555

Fig. 2. Resolved spectrum of Nd−Li−I gas complex in exp. 2. $T_{min} = 1135$ K. 1, Unresolved spectrum; 2, Difference spectrum; 3, Scaled spectrum of $NdI_3(g)$.
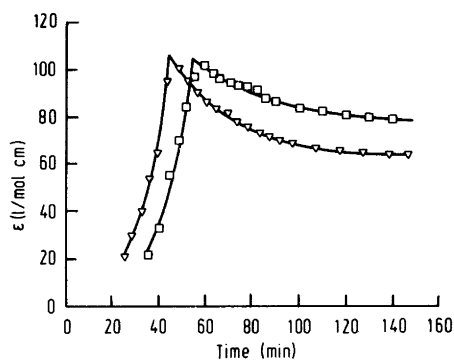

Fig. 3. Apparent molar absorption coefficient of Li −Nd−I gas complex at 16.555 kK calculated from eqn. (1) plotted *versus* time. Stable temperature corresponding to controller set points is given in parentheses. □, Exp. 4 (first 18 points) (1250 K; rest 1200 K); ∇, Exp. 5 (1216 K).

kK) calculated from eqn. (1) is plotted *versus* time for two experiments in Fig. 3. Zero time is the moment when the cell was placed in the furnace. From the figure it can be seen that the first spectra in each experiment have been recorded before all material in the cell has evaporated. As the temperature is raised, an increasing amount of the vapor complex is formed. The apparent molar absorption coefficient has a maximum when all the salt has evaporated, and decreases with further increase in temperature. The apparent molar absorption curve as function of time as shown in Fig. 3 is seen to flatten with increasing time, *i.e.* as the temperature stabilizes. Experiments performed over an extended period of time gave a nearly linear decrease in the measured values. Such behaviour is explained by a reaction with the cell material, as the reaction rate will be constant at constant temperature. Only the absorption spectrum of $I_2(g)$ was observed after about 48 h. Reaction between lanthanide triiodides and quartz has been discussed by Corbett, Sallach and Lokken.[17]

The apparent molar absorption coefficient was found by extrapolation as indicated in Fig. 3, and was taken as the ordinate of the point where the extrapolated curves cross. No temperature dependence was detected for the maximum apparent molar absorption coefficient recorded in different experiments, as seen from Table 1. The time/temperature variation is due to two processes taking place during the experiments. The reaction with quartz leads to a decreasing concentration of the vapor complex with temperature and time, and the rising temperature during an experiment gives increased thermal dissociation of the complex. The

net molar absorption coefficient at 16.555 kK was calculated from eqn. (4), when χ had been established using the band resolution method described previously. The scatter of the molar absorption coefficients obtained thus is relatively small, and the molar absorption coefficients show no dependence on temperature, as seen from Table 1. The molar absorption coefficients of the iodide complexes were therefore assumed to be independent of temperature, and were taken as the mean value of the net molar absorption coefficient. The fraction of NdI$_3$ that is not bound in the gas complex is approximately 5%. This value agrees with estimates for the CsI – NdI$_3$ system.[9] In the following calculations, the value 96.7 l/mol · cm was used for the net molar absorption coefficient of the Nd – Li – I gas complex.

B. Molar absorptivity coefficient of NdI$_3$(g)

The absorption spectrum of NdI$_3$(g) was needed for the resolution of the spectra. A part of the absorption spectrum is shown in Fig. 4. In addition to the transitions at 16.347, 16.491 and 16.624 kK, weak absorption bands were observed at 14.887 and 18.778 kK.

Experiments aimed at determining the molar absorption coefficient of NdI$_3$(g) failed, due to the reaction with quartz. The molar absorptivity at 16.347 and 16.555 kK was determined from experiments where NdI$_3$(g) was in equilibrium with NdI$_3$(l), utilizing the vapor pressure equation for liquid NdI$_3$ which has been calculated by Gruen and DeKock[8] from the data of Shimazaki and Niwa[18]

Table 1. Net molar absorptivity of Nd – Li – I gas complex at 16.555 kK. χ, Fraction of the total amount of NdI$_3$ in the molar absorptivity cell which is in equilibrium with the gas complex. k, Scaling factor, which is multiplied with the optical densities in the reference spectrum of NdI$_3$(g). A_{ref}(NdI$_3$), Optical density at 16.555 kK (A) measured for NdI$_3$(g) in separate experiments. Spectra recorded at different temperatures were used as references. ε_{app}, Apparent molar absorption coefficient of the gas complex. ε, Net molar absorption coefficient of the gas complex calculated from eqn. (4). For the molar absorption coefficient of NdI$_3$(g), $\varepsilon_{NdI_3} = 200$ l/mol cm was used at 16.555 kK.

Exp. No.	T_{min} (K)	V (cm^3)	l (cm)	m_{NdI_3} (mg)	A_{ref}(NdI$_3$)	k	χ	ε_{app} (l/mol cm)	ε (l/mol cm)	$\bar{\varepsilon}$ (l/mol cm)
1	1184	173.90	15.03	6.54	0.0255	0.524	0.062	98	91.3	
2	1225	182.65	15.23	3.39	0.0563	0.089	0.046	98	93.0	
3	1163	166.25	15.08	2.85	0.0212	0.293	0.063	105	98.6	96.7 ± 4.4
4	1143	183.54	15.26	2.37	0.0119	0.271	0.043	106	101.8	
5	1167	175.00	14.88	3.09	0.0189	0.265	0.050	104	98.9	

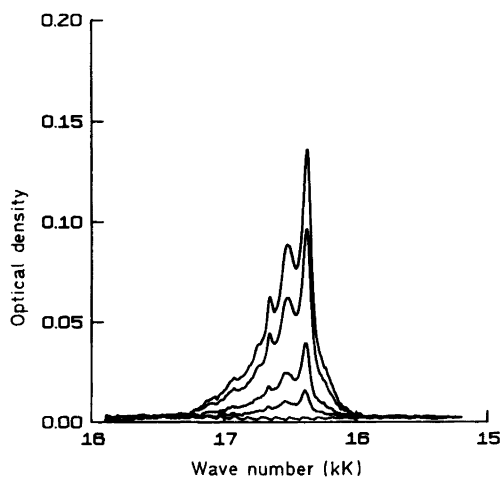*Fig. 4.* Absorption band due to the $^4I_{9/2} - {}^4G_{5/2}$ transition in $NdI_3(g)$. $T_{min}(K) = 483$, 1117, 1165, 1215, 1236.

$$RT \ln(P^\circ_{NdI_3}/atm) =$$
$$145.69T - 32.24T \log T - 70884 \qquad (6)$$

[eqn. (6)]. The molar absorption coefficients calculated at 16.347 and 16.555 kK were then 346 ± 5 and 200 ± 17 l/mol cm.

C. Gas Complexation between LiI and NdI_3

Spectra were recorded of the gas phase in equilibrium with $LiI - NdI_3$ mixtures of different compositions. Table 2 gives the experimental specifications and Fig. 5 the measured optical densities.

The logarithm of the measured optical density at the wave number of the absorption maximum is
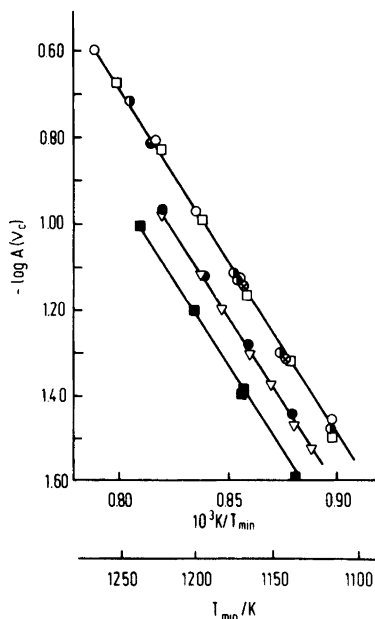

Fig. 5. Optical densities at 16.555 kK measured for the gas phase in equilibrium with $LiI - NdI_3$ liquid mixtures at various compositions. ■, Exp. 6, 10 mol% LiI. ●, Exp. 7, 20 mol% LiI. □, Exp. 8, 33 mol% LiI. ○, Exp. 9, 50 mol% LiI. ◑, Exp. 10, 50 mol% LiI. ⊗, Exp. 11, 50 mol% LiI. ∇, Exp. 12, 75 mol% LiI.

plotted *versus* inverse temperature in Fig. 5, and linear plots with the same slope are observed. The most straightforward explanation for this is that one gas complex with a temperature independent molar absorptivity is predominant at all melt compositions. When one gas complex evaporates, ln *A versus* $1/T$ will directly give the enthalpy change for the vaporization reaction if the molar absorption
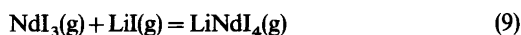
Table 2. Experimental specifications.

Exp. No.	X_{LiI}	Volume cm^3	Optical path cm	w_{NdI_3} mg	w_{LiI} mg
6	0.10	84.2	15.14	99.5	2.83
7	0.20	84.2	15.11	64.8	4.11
8	0.33	73.3	15.10	96.8	12.2
9	0.50	72.7	15.00	48.9	12.6
10	0.50	73.0	15.08	63.2	15.8
11	0.50	73.0	15.06	63.2	15.8
12	0.75	73.0	15.10	100.7	76.9

coefficient of the complex and melt composition is constant. It can be shown that the concentration change of the liquid due to the vaporization is small.

From Fig. 5 it is observed that the optical density curve has a maximum close to when the melt contain equimolar amounts of LiI and NdI_3. This indicates that $LiNdI_4(g)$ is the most probable complex gas compound in the $LiI - NdI_3$ system in accordance with what generally is found for lanthanide chloride – alkali chloride systems.[9,10]

It is hence assumed that the complex $LiNdI_4(g)$ is formed in the vapor above liquid $LiI - NdI_3$ mixtures. The following independent equilibria are considered; subscript c is used to denote the gas complex:

$$NdI_3(l) = NdI_3(g) \quad K_7 = P^\circ_{NdI_3} \tag{7}$$

$$LiI(l) = LiI(g) \quad K_8 = P^\circ_{LiI} \tag{8}$$

$$NdI_3(g) + LiI(g) = LiNdI_4(g) \tag{9}$$
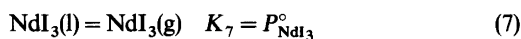
$$K_9 = \frac{P_c}{P_{LiI} P_{NdI_3}}$$

Introduction of the activity of LiI and NdI_3 in the liquid mixture, eqn. (10), gives the expression (11) for

$$a_i = P_i / P^\circ_i \tag{10}$$

$$P_c = K_7 K_8 K_9 a_{NdI_3} a_{LiI} \tag{11}$$

P_c, where K_7 and K_8 are known from previous thermodynamic studies.

The total amount of NdI_3 in the gas phase is given by eqn. (12). The observed optical density at wave

$$P^{Nd}_{tot} = P_{NdI_3} + P_c \tag{12}$$

number v_j consists similarly of two parts, eqn. (13).

$$A(v_j) = A_{NdI_3}(v_j) + A_c(v_j) \tag{13}$$

When the molar absorption coefficients $\varepsilon_{NdI_3}(v_j)$ and $\varepsilon_c(v_j)$ are known, eqn. (13) can be written in terms of the partial pressures of NdI_3 and the gas complex using eqn. (2); eqn. (14). Combination of eqns. (7), (10), (11) and (14) gives eqn. (15).

$$A(v_j) = \frac{l}{RT}\{\varepsilon_{NdI_3}(v_j)P_{NdI_3} + \varepsilon_c(v_j)P_c) \tag{14}$$

$$A(v_j) = \frac{l}{RT}a_{NdI_3}K_7\{\varepsilon_{NdI_3}(v_j) + \varepsilon_c(v_j)a_{LiI}K_8 K_9\} \tag{15}$$

We can obtain $A(v_j)$ as a function of temperature by assuming a_{NdI_3} and a_{LiI} to be temperature independent and express the unknown K_9 in terms of ΔH°_9 and ΔS°_9; eqn. (16). The T to be used in the

$$A(v_j) = \frac{l}{RT}a_{NdI_3}K_7\left(\varepsilon_{NdI_3}(v_j) + \varepsilon_c(v_j)a_{LiI}K_8 \exp\{-\frac{\Delta H^\circ_9}{RT} + \frac{\Delta S^\circ_9}{R}\}\right) \tag{16}$$

expression for K_9 is the equilibrium temperature, i.e. T_{min}. $A(v_j)$ was then fitted to the experimental data treating a_{NdI_3}, a_{LiI}, ΔH°_9 and ΔS°_9 as independent parameters although a_{NdI_3} and a_{LiI} are related through the Gibbs-Duhem equation. A general purpose model-fitting program[19] was employed, using the optical densities measured at $v_j = 16.555$ kK where $\varepsilon_{NdI_3} = 200$ l/mol cm. K_7 is given by eqn. (6) and K_8 is taken from the JANAF Tables[20] as

$$\log K_8 = 4.475 - 6.136\left(\frac{10^3}{T}\right) - 0.8257\left(\frac{10^3}{T}\right)^2 \tag{17}$$

Table 3. Activities, enthalpy and entropy change of reaction (9) calculated in fit of eqn. (16) to four parameters.

x_{LiF}	a_{NdI_3}	a_{LiI}	$-\Delta H^\circ_9$ (kJ/mol)	$-S^\circ_9$ (J/mol K)	σ (%)
0.10	0.81	0.01	212.1	115.1	2.4
0.20	0.62	0.02	219.9	116.3	1.3
0.33	0.39	0.08	208.7	110.5	2.1
0.50	0.23	0.25	211.2	115.1	3.3
0.75	0.07	0.62	209.0	118.4	4.8

Table 4. Activities of NdI_3 and LiI calculated from eqn. (16) with $\Delta H_9^\circ = -210.3$ kJ/mol, $\Delta S_9^\circ = -115.5$ J/mol K, and the same activities calculated from eqns. (23)−(25) with $K_{19} = 1.5$. σ is the standard deviation in fit for eqn. (16).

x_{LiI}	a_{NdI_3} (Eqn. 16)	a_{NdI_3} (Eqn. 24)	a_{LiI} (Eqn. 16)	a_{LiI} (Eqn. 25)	σ (%)
0.10	0.80	0.81	0.01	0.006	1.7
0.20[a]	0.62	0.59	0.02	0.03	1.3
0.33	0.43	0.40	0.11	0.12	1.5
0.50	0.21	0.23	0.24	0.26	3.0
0.75	0.06	0.05	0.62	0.63	4.6

[a] Values calculated from the four-parameter fit.

The initial fit of eqn. (16) to the experimental data gave the numerical values and per cent standard deviation in fit which are given in Table 3. The values of ΔH_9° and ΔS_9° have the expected constancy, and calculation of the mean values gives a standard deviation of ± 2.1 % in ΔH_9° and ± 2.5 % in ΔS_9°. The mean values of ΔH_9° and ΔS_9° are $\Delta H_9^\circ = -210.3$ kJ/mol and $\Delta S_9^\circ = -115.5$ J/mol K. (The experiment at $X_{LiI} = 0.20$ has been omitted from the calculation, as the optimum fit of eqn. (16) to the experimental data was not achieved for this experiment.) As the second step in the calculation of thermodynamic data, these values were inserted in eqn. (16) and only the activities were treated as parameters. The results obtained from a fit of eqn. (16) to the experimental data using the mean values given above are given in Table 4. As expected, this calculation gave only minor changes of the activities compared with the results given in Table 3.

The thermodynamic functions for reaction (9) $\Delta H_9^\circ = -210.3$ kJ/mol and $\Delta S_9^\circ = -115.5$ J/mol K have reasonable values. ΔS_9° is within the limit -125 ± 20 J/mol K expected for a reaction of this type.[3] ΔS_9° is about 10 J/mol K more negative than ΔS° reported for the corresponding reaction to $CsNdI_4$[9] which compares well with the 10 % increase in the entropy of formation of $CsNdCl_4$[11] relative to $LiNdCl_4$.

ΔH_9° is 28 kJ less negative than the corresponding reaction to give $CsNdI_4$,[9] so that both the entropy and enthalpy change from $CsNdI_4$ to $LiNdI_4$ predict a lower stability of the $LiNdI_4$ complex. This parallels the observation made by Linga *et al.*[21] for the series $LiAlCl_4 - NaAlCl_4 - KAlCl_4$. Schäfer and Wagner[22-26] found the same increase in the stability of $MScCl_4$ vapor complexes when M was changed from Li to Cs. Reported data for $MNdCl_4(g)$[11] and $MGdCl_4(g)$[27] (M = Li, Na, K, Cs) show an opposite stability trend.

D. Complexation in Liquid $NdI_3 - LiI$ Mixture

The analysis of the gas complexation data did not only give the thermodynamics for this reaction, but also the activities of LiI and NdI_3 in the liquid mixtures (Table 4). In order to complete the thermodynamic treatment, it is of interest to attempt to describe the liquid activities in terms of a model and simultaneously test that the independently calculated activities are consistent with the Gibbs-Duhem equation.

The strong negative deviation from ideality indicate complex formation also in the liquid phase, and the presence of MI_6^{3-} ion has been suggested.[28] As the coordination of NdI_3 in pure liquid NdI_3 also probably is 6, a model parallel to that proposed by Førland[29] for $MgCl_2 - KCl$ may be introduced.

An equilibrium between three types of I^- ions is considered; *i.e.*, end I^-, bridged I^- and free I^-.

$$2[-I-Nd\!\!\overbrace{-I\,]}^{-0.5} =$$

$$[-I-Nd\!\!\overbrace{-I\,}\!\!-Nd-I-]+[\,I\,]^{-1} \qquad (18)$$
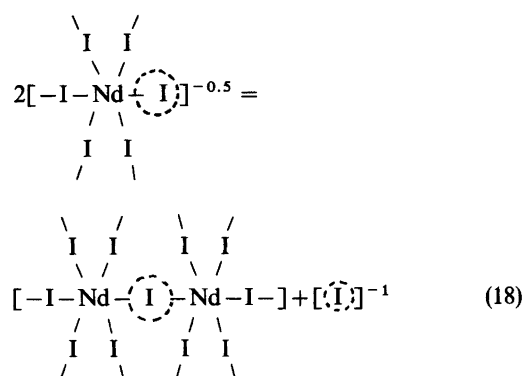
This equilibrium can be written in an abbreviated form as eqn. (19). The equilibrium expression is given as eqn. (20), where X is mol fraction; n number of mol; and b: bridge; f: free and e: end.

$$2I_e^{-0.5} = I_b + I_f^{-1} \tag{19}$$

$$\frac{n_{I_b} n_{I_f}}{(n_{I_e})^2} = \frac{X_{I_b} X_{I_f}}{(X_{I_e})^2} = K_{19} \tag{20}$$

Using 1 mol of LiI — NdI$_3$ mixture as basis, the mass balance and electroneutrality requirements are given by eqns. (21) — (22). Combination of eqns. (20) — (22) gives eqn. (23).

$$n_{I_b} + n_{I_f} + n_{I_e} = 2X_{NdI_3}^\circ + 1 \tag{21}$$

$$0.5 n_{I_e} + n_{I_f} = 1 - X_{NdI_3}^\circ \tag{22}$$

$$\frac{(4X_{NdI_3}^\circ - 1 + n_{I_f}) n_{I_f}}{(1 - X_{NdI_3}^\circ - n_{I_f})^2} = 4K_{19} \tag{23}$$

As we have introduced the restriction of one mol of mixture and as no exchange between Li and Nd is assumed (*i.e.* Li$^+$ is the only cation), the simplest activity model for LiI is given by eqn. (24). The activity of NdI$_3$ is obtained by the use of the Gibbs-Duhem equation, eqn. (25)

$$a_{LiI} = n_{I_f} \tag{24}$$

$$a_{NdI_3} = -\int_0^{n_{I_f}} \frac{X_{LiI}}{X_{NdI_3}} \, d\ln n_{I_f} \tag{25}$$

K was then varied and a least squares fit of the activities of LiI and NdI$_3$ was performed. From Fig. 6 it is seen that this one-parameter model gives a quite satisfactory description of the experimental
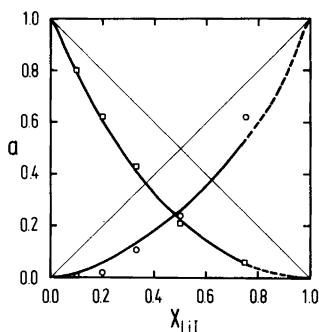
Fig. 6. a_{NdI_3} and a_{LiI} *versus* composition of the LiI — NdI$_3$ melts. $\square$, a_{NdI_3}, $\bigcirc$, a_{LiI} calculated from eqn. (16). The lines are the activities of LiI obtained from model calculation [eqns. (23) — (24)] and the corresponding a_{NdI_3} using Gibbs-Duhem's equation (eqn. 25).
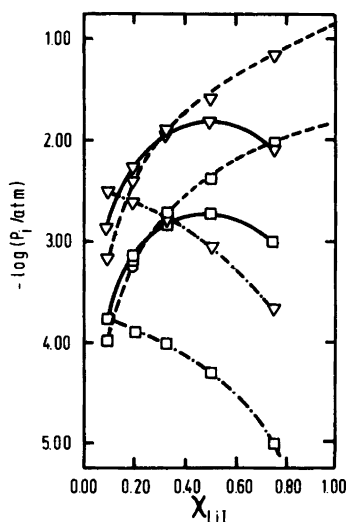
Fig. 7. Calculated partial pressures of LiNdI$_4$, NdI$_3$ and LiI above liquid LiI — NdI$_3$ mixtures at $\square$, 1100 K and $\triangledown$, 1250 K. — · —, NdI$_3$; – – –, LiI; ——, LiNdI$_4$.

data with $K_{19} = 1.5$ and that the required consistency check by use of Gibbs-Duhem equation is fulfilled.

The only appreciable deviation is a_{LiI} for $X_{LiI} = 0.75$ but this may just as well be due to experimental uncertainties (compare standard deviations in Table 4) as due to failure of the model.

Finally Fig. 7 gives the partial pressures of LiI, NdI$_3$ and LiNdI$_4$. The partial pressure of LiNdI$_4$ is lower than that of CsNdI$_4$ due to the larger stability of the latter complex. The volatility enhancement of NdI$_3$ can be given by the expression (26).

$$v_r = (P_{LiNdI_4} + P_{NdI_3})/P_{NdI_3}^\circ \tag{26}$$

P_{LiNdI_4} and P_{NdI_3} are the partial pressures of the gas complex and NdI$_3$, and $P_{NdI_3}^\circ$ is the vapor pressure of liquid NdI$_3$. The volatility enhancement at 1100 K is 7.5, and 3.3 at 1250 K, and shows that the complex formation gives a significant increase in the transport of NdI$_3$ to the gas phase in spite of the lower stability of LiNdI$_4$ *versus* CsNdI$_4$.

REFERENCES

1. Øye, H. A. and Gruen, D. M. *J. Am. Chem. Soc.* 91 (1969) 2229.

2. Emmenegger, F. P. *J. Cryst. Growth 17* (1972) 31.
3. Hastie, J. W. *High Temperature Vapors-Science and Technology*, Academic, New York 1975.
4. Schäfer, H. *Angew. Chem. 23* (1976) 775.
5. Øye, H. A. and Gruen, D. M. In Hastie, J. W., Ed., *Characterization of High Temperature Vapors and Gases*, (NBS 10. Materials Research Symposium), NBS Special Publ. 561, Washington D.C. 1979, Vol. 1, p. 1517.
6. Funk, W., Hartel, G. and Kloss, H. G. *Beitr. Plasmaphys. 11* (1971) 179.
7. Dobrusskin, A. *Light. Res. Technol. 3* (1971) 125.
8. Gruen, D. M. and DeKock, C. W. *J. Chem. Phys. 45* (1966) 455.
9. Liu, C. S. and Zollweg, R. J. *J. Chem. Phys. 60* (1974) 2384.
10. Hirayama, C., Liu, C. S. and Zollweg, R. J. In Cubicciotti, D. and Hildenbrand, D. L., Eds., *High Temperature Metal Halide Chemistry*, The Electrochemical Society Softbound Symposium Series, Princeton, N.J. 1977, p. 95.
11. Novikov, G. I. and Gavryuchenkov, F. G. *Russ. Chem. Rev. 36* (1967) 156.
12. Gavryuchenkov, F. G. and Novikov, G. I. *Russ. J. Inorg. Chem. 11* (1966) 810.
13. Novikov, G. I. and Gavryuchenkov, F. G. *Russ. J. Inorg. Chem. 10* (1965) 909.
14. Novikov, G. I. and Baev, A. K. *Russ. J. Inorg. Chem. 9* (1964) 905.
15. Borgen, O., Bruvoll, T. and Petersen, H. *A Data Collection and Recording System for the CARY 17H Spectrophotometer*, Technical Report 70, Division of Physical Chemistry, University of Trondheim, NTH, Trondheim 1976.
16. Anundskås, A. and Øye, H. A. *J. Inorg. Nucl. Chem. 37* (1975) 1609.
17. Corbett, J. D., Sallach, R. A. and Lokken, D. A. *Adv. Chem. Ser. 71* (1967) 56.
18. Shimazaki, E. and Niwa, K. *Z. Anorg. Allg. Chem. 314* (1962) 21.
19. Hertzberg, T. *"MODTLP" Report*, Institutt for kjemiteknikk, NTH, Trondheim 1970.
20. *JANAF Thermochemical Tables*, 2nd Ed., NSRDS-NBS 37, US Dept. of Commerce, Washington, D.C. 1971
21. Linga, H., Motzfeldt, K. and Øye, H. A. *Ber. Bunsenges. Phys. Chem. 82* (1978) 568.
22. Schäfer, H. and Wagner, K. *Z. Anorg. Allg. Chem. 450* (1979) 88.
23. Wagner, K. and Schäfer, H. *Z. Anorg. Allg. Chem. 450* (1979) 107.
24. Wagner, K. and Schäfer, H. *Z. Anorg. Allg. Chem. 450* (1979) 115.
25. Wagner, K. and Schäfer, H. *Z. Anorg. Allg. Chem. 451* (1979) 57.
26. Schäfer, H. and Wagner, K. *Z. Anorg. Allg. Chem. 451* (1979) 61.
27. Dientsbach, F. and Blachnik, R. *Z. Anorg. Allg. Chem. 442* (1978) 135.
28. Kutscher, J. *Dissertation*, Fakultät für Natur- und Geisteswissenschaften der Technischen Universität Clausthal, BRD 1972.
29. Førland, T. In Sundheim, B. R., Ed., *Fused Salts*, McGraw-Hill, New York 1964, p. 145.